Quantum Monte Carlo Simulation of the Davydov Model

Xidi Wang,[a] David W. Brown,[b] and Katja Lindenberg[b],[c]
University of California, San Diego, La Jolla, California 92093
(Received 21 November 1988)

Through an application of the quantum Monte Carlo technique, we investigate the thermal equilibrium properties of the one-dimensional model proposed by Davydov for the description of energy transport processes in the α helix. The deformation of the lattice about a single (moving) excitation is computed over a wide range of temperatures. We find that the model does admit a coherent structure at low temperatures, but that this structure is substantially destroyed above 7 K.

PACS numbers: 87.22.−q, 71.38.+i, 71.50.+t, 72.15.Rn

Extensive effort in recent years has been brought to bear on examining the possibility of energy transport in 1D molecular systems by a soliton mechanism as proposed by Davydov.[1,2] Exact solutions for the model Hamiltonian [cf. (1)] are unavailable except in a few limiting cases, and the accuracy of numerical simulations has been limited by their basis in equations of motion derived from the Davydov *Ansatz* wave functions ("D_1" and "D_2" as distinguished in Ref. 3). Though progress has been made in understanding the approximate nature of these *Ansätz,* no quantitative characterization of the error involved in their use is known. Using D_2 *Ansatz* machinery, Refs. 4 and 5 find stable solitons at zero temperature in the standard 1D α-helix model, while Refs. 5 and 6 find that the soliton appears to be unstable at room temperature. Using D_1 *Ansatz* machinery, Cruzeiro *et al.*[7] claim solitons can still survive at room temperature. In interpreting finite-temperature dynamical simulations one must resolve any solitons which may be present against a noisy background consisting of thermal fluctuations and radiation emitted during the relaxation of initial states. Characterization of solitons in such an environment is difficult. In practice, qualitative characterizations are made on the basis of a relatively small number of runs perceived as being representative of an ensemble.

We present results of numerical simulations based on the quantum monte carlo (QMC) technique first proposed by Suzuki, Miyashita, and Kuroda.[8] The QMC technique is not limited by formal approximations; the accuracy of the equilibrium expectation values computed is limited only by grid-size effects and statistical errors due to limited run times. Subject only to these limitations, the results we report are definitive.

The Hamiltonian proposed by Davydov and Kisluka[1,2] as a model for vibrational excitations of the α helix is a Fröhlich-type Hamiltonian:

$$\hat{H}=\sum_i E a_i^\dagger a_i - J\sum_i (a_{i+1}^\dagger a_i + a_i^\dagger a_{i+1}) + \sum_i \left[\frac{\hat{P}_i^2}{2M} + \frac{w}{2}(\hat{Q}_{i+1}-\hat{Q}_i)^2\right] + \chi\sum_i (\hat{Q}_{i+1}-\hat{Q}_{i-1}) a_i^\dagger a_i , \tag{1}$$

where $a_i^\dagger, a_i$ are boson creation and annihilation operators of C=O bond excitation on the ith site of the α helix and $\hat{P}_i, \hat{Q}_i$ are the momentum and position operators of the center of mass of the ith peptide group in the polypeptide chain. E is the site energy, J is the transfer matrix element, M is the mass of each polypeptide group, w is the longitudinal stiffness coefficient, and χ is the force exerted by an excitation on nearest-neighbor molecules. We focus on the one-excitation Davydov model although the calculation for the many-excitation case can be carried out in essentially the same way.

In the canonical ensemble, the thermal equilibrium expectation value of any physical observable $\hat{O}$ is given by

$$\langle \hat{O} \rangle = \mathrm{Tr}(\hat{O} e^{-\beta \hat{H}}) / \mathrm{Tr}(e^{-\beta \hat{H}}) . \tag{2}$$

Following Ref. 8, (2) is formulated in terms of Feynman's path integral for the quantum propagator with *imaginary time* β, and the canonical weights are generated by importance sampling of the possible quantum paths. We compute the partition function $Z=\mathrm{Tr}(e^{-\beta \hat{H}})$ by first dividing the imaginary time β into L intervals $\Delta\tau=\beta/L$. Between each pair of intervals we then insert a complete set of basis states, thereby representing all L-polygonal arcs through the Hilbert space connecting the initial and final imaginary times. Our basis states are products of exciton number states and the position eigenstates of the lattice. Using the *checkerboard decomposition* technique,[9] we separate the Hamiltonian (1) into two parts, $\hat{H}=\hat{H}_2\{\hat{P}\}+\hat{H}_1\{\hat{Q}\}$, such that $\hat{H}_2\{\hat{P}\}$ contains all lattice momentum operators $\hat{P}$ and all exciton hopping terms from *even*-numbered sites, and $\hat{H}_1\{\hat{Q}\}$ contains all lattice position operators together with all exciton hopping terms from *odd*-numbered sites. The Trotter formula

$$e^{-\Delta\tau \hat{H}} = e^{-\Delta\tau \hat{H}_2\{\hat{P}\}} e^{-\Delta\tau \hat{H}_1\{\hat{Q}\}} [1+O\{\Delta\tau^2\}]$$

allows Z to be approximated by

$$Z \approx \int \prod_{i,j} dQ_{ij} \exp\left\{ -\Delta\tau \sum_{i,j} \left[\frac{M}{2} \left(\frac{Q_{i,j+1} - Q_{i,j}}{\Delta\tau} \right)^2 + \frac{w}{2} (Q_{i+1,j} - Q_{i,j})^2 \right] \right\}$$
$$\times \mathrm{Tr} \prod_{j=1}^{L} \exp\left(+\Delta\tau J \sum_{i \text{ even}} (a_{i+1}^{\dagger} a_i + a_i^{\dagger} a_{i+1}) \right)$$
$$\times \exp\left(-\Delta\tau \sum_{i \text{ odd}} \{ \chi [(Q_{i+1,j} - Q_{i-1,j}) a_i^{\dagger} a_i + (Q_{i+2,j} - Q_{i,j}) a_{i+1}^{\dagger} a_{i+1}] - J (a_{i+1}^{\dagger} a_i + a_i^{\dagger} a_{i+1}) \} \right), \quad (3)$$

wherein $Q_{i,j}$ is the position of the ith lattice mass at the jth cut. For sufficiently small $\Delta\tau$, higher-order terms in the Trotter formula can be neglected.[10] In order to compute the trace in (3) we need only diagonalize the dimer problem appearing inside the trace operator. The dimers are decoupled (thanks to the checkerboard decomposition), allowing the needed matrix elements to be calculated analytically prior to simulation.

Equation (3) is the basis of our QMC simulation. The summation in (3) is over all possible *world line* configurations[9] determined by the intermediate states inserted in the partition function. The product of all terms of Z along a particular world line gives the weight with which that path occurs in the canonical ensemble. In principle this weight could be calculated in its entirety. In fact, however, we calculate this weight in a much simpler way: Following the initialization of the first accepted world line configuration, we generate new world lines by making tentative *local* changes of an existing world line in a random fashion (as in Ref. 9). We use the heat-bath algorithm[11] for sampling the exciton part of the world line, and the Metropolis algorithm[12] for sampling the lattice part of the world line. The only quantities actually calculated are ratios of *local* quantities where a tentative change has been made; thus, the global calculation that (3) appears to require for each world line configuration is reduced to a local calculation, and the amount of computation is dramatically reduced.

There are a number of situations where the accuracy of the program can be tested. The simplest test cases are the decoupled exciton and lattice systems. Our lattice dynamics has been tested by computing probability distributions for individual oscillators,[12] and comparing the results with exact ground states. Our free-exciton calculation has been tested by computing the imaginary-time density correlation function $\langle n(i,0) n(i+l,\tau) \rangle$, deriving from this free-exciton effective mass[9] and comparing the result with the theoretical effective mass $\hbar^2/2Jl^2$. The coupled system has been tested in the limit $J \to 0$. The lattice deformation was measured (cf. below), and compared with the exact analytical result.[13] In all testing procedures simulation results were found to agree with theoretical values to within a few percent. (A typical series of runs averaged over 20000 measurements after 2000 warmup sweeps, with $\Delta\tau = 0.2$. Smaller values of $\Delta\tau$ showed no significant improvement in accuracy.)

There are no exact solutions available against which to check our simulation of the fully interacting system; however, there is one quantity whose equilibrium expectation value is independent of J, T, and N.[14] That quantity is the net contraction of the lattice, defined for free boundary conditions (fbc) as

$$\langle \Delta\hat{Q} \rangle \equiv \langle \hat{Q}_N \rangle - \langle \hat{Q}_1 \rangle = -2\chi/w , \quad (4)$$

or equivalently as the sum of all local contractions $\langle \Delta\hat{Q}_n \rangle \equiv \langle \hat{Q}_{n+1} \rangle - \langle \hat{Q}_{n-1} \rangle$. We used periodic boundary conditions (pbc), which cause each local contraction to be modified such that

$$\langle \Delta\hat{Q}_n \rangle_{\mathrm{pbc}} = \langle \Delta\hat{Q}_n \rangle_{\mathrm{fbc}} - N^{-1} \langle \Delta\hat{Q} \rangle_{\mathrm{fbc}} .$$

The value of the free boundary lattice contraction can be derived from the dependence of $\langle \Delta\hat{Q}_n \rangle_{\mathrm{pbc}}$ on n and used to monitor the accuracy of the simulation. In every QMC run, the net lattice contraction was verified to agree with the theoretical value (4) to within a few percent.

Because of the translational invariance of the Hamiltonian, the thermal-equilibrium probability of an excitation appearing on any given lattice site is independent of the choice of site, and thus the average lattice deformation at any particular lattice site is zero (apart from the net lattice contraction noted above). To measure the deformation around the excitation, we must construct a correlation function using a *moving coordinate* as in Ref. 9. A measurement is made by detecting the excitation on, say, the mth site. Having determined the location of the excitation, we then measure the configuration of the lattice relative to this site, and ensemble average this lattice configuration. Thus

$$C_i = \left\langle \sum_j n_{m,j} (Q_{m+i+1,j} - Q_{m+i-1,j}) \right\rangle , \quad (5)$$

where $n_{m,j}$ is zero or one, depending on the location of the excitation at the jth cut, and $\langle \cdots \rangle$ indicates the average over all runs. Simulation results for C_i using the α-helix parameters of Table I are shown in Fig. 1 for a number of temperatures. We terminated our survey at $T = 0.27$ K, a temperature well below the 13.6 K which corresponds to the soliton binding energy predicted by Davydov.[2] Lower-accuracy runs at lower temperatures showed little deviation from the $T = 0.27$-K results.

Figure 1 offers clear evidence that at low temperatures the excitation and the lattice participate cooperatively in a coherent structure, the basic unit of which extends over 2–3 sites. This bell-shaped structure is not consistent

TABLE I. Model parameters for the α helix as given in Ref. 15. The site energy E plays no role in our calculation and so has been neglected.

Parameter	Value	Unit
J	7.8	cm^{-1}
l	5.4	Å
M	114	m_p
w	13	$N\ m^{-1}$
χ	6.2×10^{-11}	N

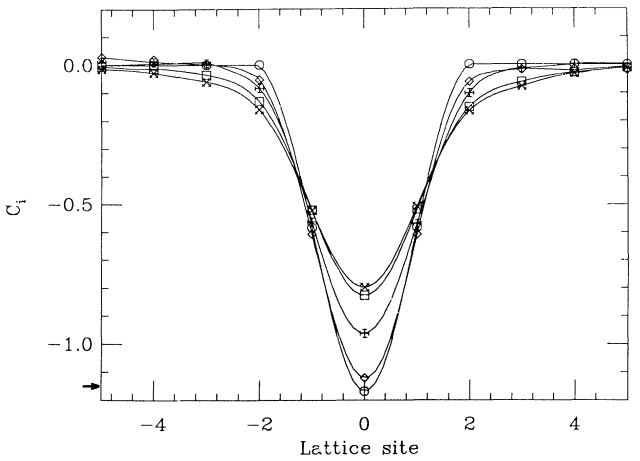

FIG. 1. Simulation results for the deformation function C_i [cf. (5)] using the α-helix parameters of Table I. ×, $T=0.27$ K; □, $T=2.8$ K; +, $T=7.0$ K; ◇, $T=11.2$ K; and ○, $T=\infty$. The latter data are obtained by examining the QMC algorithm and observing that the only possible result of a QMC survey at infinite temperature is that displayed. The vertical axis is in simulation units. The arrow indicates the value of C_0 at infinite temperature, 9.5×10^{-2} Å, or 1.76% of the lattice constant. Only eleven lattice sites are shown; however, every QMC run was made on a lattice of at least 24 sites. Solid lines through the data are provided to aid the eye only; no theoretical fit has been performed to obtain these curves.

with the common picture of the sech soliton of the (continuum) nonlinear Schrödinger equation, but it is roughly consistent with the results of the *modified* nonlinear Schrödinger equation which contains corrections due to the discreteness of the lattice .[16] With increasing temperature, thermal fluctuations compete with increasing effectiveness against the forces maintaining the coherent structure, such that at high temperatures coherence cannot be maintained even between nearest-neighbor sites. The result is the erosion of the basic unit of the coherent structure toward a localized state, and the disintegration of the whole coherent structure into a superposition of localized states. The nearness of our 11.2-K results to the infinite-temperature result suggests that the destruction of the coherent structure is essentially complete at 11.2 K. The center of the transition appears to fall at 7 K, corresponding to an energy approximately half of the soliton binding energy predicted by Davydov.

Fixed-temperature surveys were also carried out by varying the coupling constant χ. Unlike temperature surveys, which show the width of the lattice deformation to decrease monotonically with increasing temperature, the fixed-temperature lattice deformation was found to have a maximum width at intermediate coupling strengths. Below the transition into the weak-coupling regime, thermal fluctuations are sufficiently strong to be effective in degrading the coherent structure, and decreases in coupling strength result in progressive localization due to loss of coherence, as discussed above. In the strong-coupling regime, the binding energy is too large for thermal fluctuations to have any serious effect, and the narrowing of the deformation with increasing coupling strength is due to increasing coherence.

A typical (0.27 K) world line configuration for α-helix parameters is shown in Fig. 2. Fluctuations in the lattice configurations are primarily due to the zero-point motion of the masses, thermal fluctuations are very small, and the amplitude of the lattice deformation is only a fraction of the amplitude of the quantum fluctuations. The strong quantum fluctuations in the lattice are due to the acoustic nature of the phonons. Each normal mode of frequency ω_q contributes $O\{\hbar/2NM\omega_q\}$ to the mean-square amplitude $\langle 0|\hat{Q}_n^2|0\rangle$; consequently, long-wavelength acoustic modes contribute strongly to zero-point motion. Though the importance of zero-point motion depends on a number of factors including system size and dimension, this Goldstone-mode nature of acoustic phonons is expected to be present.[17] A limited test of the role of quantum fluctuations in the lattice can be made by varying the lattice mass M. We increased M by a factor of 100 at $T=0.35$ K and observed the deformation to be essentially unchanged apart from a small (few percent) increase in width, suggesting that despite their large amplitude, quantum fluctuations have only a small effect on the equilibrium deformation.

Our quantum Monte Carlo simulation of the Davydov model of energy transport in the α helix has yielded several conclusions: (1) A coherent structure exists for temperatures below 7 K; (2) the basic unit of this coherent structure is highly localized and bears a close resemblance to the Davydov soliton if discreteness corrections to the latter are taken into account; and (3) above 7 K thermal fluctuations are effective in destroying the internal coherence of this basic unit, its destruction being essentially complete above 11.2 K. These results are largely consistent with the dynamical simulations of Lomdahl and Kerr[5] based on D_2 *Ansatz* states. A major difference is that we find quantum fluctuations, absent from Ref. 5, to be quite strong (cf. Fig. 2). The *equilibrium* quantity we have presented is not seriously affected by quantum fluctuations, but it is likely that *dynamical* properties would be affected by the presence of intrinsic quantum noise.

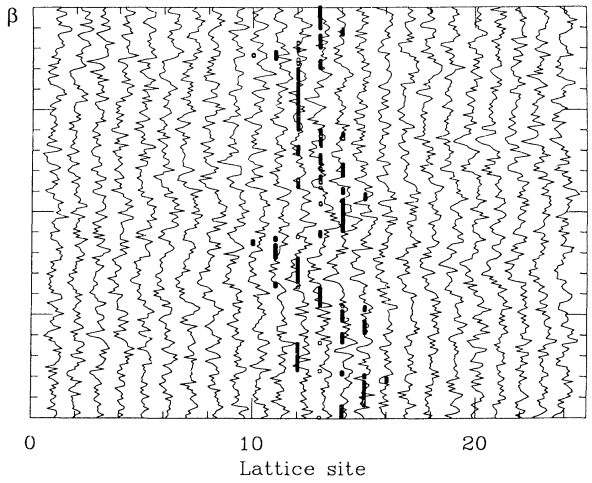

FIG. 2. A typical world line configuration for α-helix parameters at 0.27 K. In this simulation, β has been subdivided into 400 cuts. Vertices of the polygonal arcs represent the value at each cut of the deviation $Q_n - R_n$ from its free-lattice equilibrium position position R_n. (The size of these deviations has been magnified by a factor of 30 for ease of viewing.) Similarly, open circles represent the location of the excitation at each cut. There may appear to be more than one excitation present at a particular cut despite the fact that every cut contains exactly one excitation. This illusion is due to occasional rapid (in β) oscillations of the excitation between adjacent sites, which are difficult for the eye to resolve due to the high density of cuts. Careful comparison of an occupied and an unoccupied region shows how the weak, average deformation of Fig. 1 is realized amidst a sea of intrinsic quantum noise.

Our results characterize only the basic unit from which the state of the system is built up by linear superposition, and thus our characterization of the quantum state of the system is necessarily incomplete. It is clear, however, that the nonlinear coherence which distinguishes solitons from other quasiparticles is present in this system at low temperature. Our low-temperature results therefore appear to favor a soliton superposition state such as that of Venzl and Fischer.[18] Above 7–11 K the apellation "soliton" appears to have little meaning, and a description in terms of small-polaron states may be quite adequate.

The authors thank Professor Jorge Hirsch for constructive suggestions at numerous stages in the development and implementation of our QMC algorithm, and the Institute for Nonlinear Science at the University of California, San Diego, for computer time and support. This work was supported in part by U.S. Defense Advanced Research Projects Agency, Contract No. DAAG-29-K-0246, and by NSF Grant No. DMR 86-19650-A1.

[a]Department of Physics, B-019.
[b]Institute for Nonlinear Science, R-002.
[c]Department of Chemistry, B-040.

[1]A. S. Davydov and N. I. Kislukha, Phys. Status Solidi **59**, 465 (1973); Zh. Eksp. Teor. Fiz. **71**, 1090 (1976) [Sov. Phys. JETP **44**, 571 (1976)].

[2]A. S. Davydov, Phys. Scr. **20**, 387 (1979); Usp. Fiz. Nauk. **138**, 603 (1982) [Sov. Phys. Usp. **25**, 898 (1982)]; Zh. Eksp. Teor. Fiz. **51**, 789 (1980) [Sov. Phys. JETP **78**, 397 (1980)].

[3]David W. Brown, Katja Lindenberg, and Bruce J. West, Phys. Rev. A **33**, 4110 (1986); **33**, 4014 (1986).

[4]A. C. Scott, Phys. Scr. **29**, 279 (1984); L. MacNeil and A. C. Scott, Phys. Scr. **29**, 284 (1984).

[5]P. S. Lomdahl and W. C. Kerr, Phys. Rev. Lett. **55**, 1235 (1985); in *Physics of Many Particle Systems,* edited by A. S. Davydov, (Naukova Dumka, Kiev, 1988).

[6]Albert F. Lawrence, James C. McDaniel, David B. Chang, Brian M. Pierce, and Robert R. Birge, Phys. Rev. A **33**, 1188 (1986).

[7]L. Cruzeiro, J. Halding, P. L. Christiansen, O. Skovgaard, and A. C. Scott, Phys. Rev. A **37**, 880 (1988).

[8]M. Suzuki, S. Miyashita, and A. Kuroda, Prog. Theor. Phys. **58**, 1377 (1977).

[9]J. E. Hirsch, R. L. Sugar, D. J. Scalapino, and R. Blankenbecler, Phys. Rev. B **26**, 5033 (1982).

[10]M. Suzuki, Commun. Math. Phys. **51**, 183 (1976).

[11]See, e.g., J. W. Negele and H. Orland, *Quantum Many-Particle Systems* (Addison-Wesely Reading, MA, 1988).

[12]M. Creutz and B. Freedman, Ann. Phys. (N.Y.) **132**, 427 (1981).

[13]David W. Brown, Katja Lindenberg, and Bruce J. West, J. Chem. Phys. **84**, 1574 (1986) **87**, 6700 (1987).

[14]Xidi Wang, David W. Brown, and Katja Lindenberg (to be published).

[15]A. C. Scott, Philos. Trans. Roy. Soc. London A **315**, 423 (1985).

[16]Xidi Wang, David W. Brown, Katja Lindenberg, and Bruce J. West, Phys. Rev. A **37**, 3557 (1988).

[17]T. D. Holstein and L. A. Turkevich, Phys. Rev. B **38**, 1901 (1988).

[18]Gerd Venzl and Sighart F. Fischer, J. Chem. Phys. **81**, 6090 (1984); Phys. Rev. B **32**, 6437 (1985).